DMD Fast Forward. Published on June 17, 2011 as DOI: 10.1124/dmd.111.038588
DMD Fast Forward. Published on June 17, 2011 as doi:10.1124/dmd.111.038588
This article has not been copyedited and formatted. The final version may differ from this version.

DMD #38588

Preclinical Disposition (in vitro) of Novel μ-Opioid Receptor Selective Antagonists

Pallabi Mitra, Jürgen Venitz, Yunyun Yuan, Yan Zhang, Phillip M. Gerk

Departments of Pharmaceutics (PM, JV, PMG) and Medicinal Chemistry (YY, YZ)

Virginia Commonwealth University School of Pharmacy

Downloaded from dmd.aspetjournals.org at ASPET Journals on April 17, 2024

Copyright 2011 by the American Society for Pharmacology and Experimental Therapeutics.

DMD Fast Forward. Published on June 17, 2011 as DOI: 10.1124/dmd.111.038588
This article has not been copyedited and formatted. The final version may differ from this version.

Running Title: Preclinical Disposition of NAP & NAQ

Corresponding Author:

Phillip M. Gerk, Pharm.D., Ph.D.

Dept. of Pharmaceutics, School of Pharmacy, Virginia Commonwealth University

410 N. 12th Street, PO Box 980533

Richmond, VA 23298-0533

phone: (804) 828-6321

fax: (804) 828-8359

email: pmgerk@vcu.edu

Text Pages	24
Figures	3
Tables	2
References	35
Word Counts	
Abstract	239
Introduction	483
Discussion	1257

Non-Standard Abbreviations

ACN	acetonitrile
CL_{hep}	hepatic clearance

Downloaded from dmd.aspetjournals.org at ASPET Journals on April 17, 2024

DMD Fast Forward. Published on June 17, 2011 as DOI: 10.1124/dmd.111.038588
This article has not been copyedited and formatted. The final version may differ from this version.

CL_{int}	intrinsic clearance
CYP	cytochrome P450
DMEM	Dulbecco's Modified Eagle's Medium
DMSO	dimethylsulfoxide
HLM	human liver microsomes
HPLC	high-performance liquid chromatography
IVIVE	in vitro-in vivo extrapolation
MM	Michaelis-Menten
MOR	μ-opioid receptor
NAP	(17-cyclopropylmethyl-3,14β-dihydroxy-4,5α-epoxy-6β-[(4'-pyridyl)acetamido]morphinan)
NAQ	17-cyclopropylmethyl-3,14β-dihydroxy-4,5α-epoxy-6α-[(3'-isoquinolyl) acetamido]morphinan)
NTX	naltrexone
PDR	permeability directional ratio
P-gp	P-glycoprotein; multidrug resistance transporter 1; gene symbol *ABCB1*
UDPGA	UDP-glucuronic acid
UGT	UDP-glucuronosyltransferase

Downloaded from dmd.aspetjournals.org at ASPET Journals on April 17, 2024

DMD Fast Forward. Published on June 17, 2011 as DOI: 10.1124/dmd.111.038588
This article has not been copyedited and formatted. The final version may differ from this version.

Abstract

Recently, two novel N-heterocyclic derivatives of naltrexone, (designated NAP and NAQ) have been proposed as μ opioid receptor (MOR) selective antagonists. The goal of this study was to examine their absorption and metabolism. The bidirectional transport of NAP and NAQ was determined in Caco-2 and MDCKII-MDR1 cells, and the permeability directional ratio (PDR) was estimated (PDR = $P_{app,B-A}/P_{app,A-B}$). Oxidative metabolism of NAQ (0.5-80 μM) and NAP (0.5-30 μM) was determined in pooled human liver microsomes. The reaction monitored the disappearance of NAQ/NAP. NAP and NAQ were quantitated by HPLC-UV at 270 nm or 232 nm, respectively. The permeability of NAQ or NAP was similar to that of naltrexone or paracellular markers, respectively. NAP also exhibited a high PDR, and was determined to be a P-gp substrate. Unbound fractions in human plasma for NAQ and NAP were 0.026±0.019 and 0.85±0.12, respectively. The metabolic oxidative reaction rates, fitted to a Michaelis-Menten model, yielded K_m and V_{max} values of 15.8±5.5μM, 192±24 pmol/min for NAQ; and 1.8±1.5μM, and 8.1±1.4 pmol/min for NAP. Intrinsic hepatic clearance was estimated to be 13 and 5 mL/min/kg for NAQ and NAP, respectively. Neither NAQ nor NAP underwent detectable glucuronidation. Thus, NAP was a Pgp substrate with low apparent permeability while NAQ was not a Pgp substrate and showed better permeability. Therefore, in contrast to NAP, NAQ would be more suitable for oral absorption and penetration of the blood-brain barrier, yielding potential pharmacokinetic and pharmacodynamic advantages over naltrexone.

Downloaded from dmd.aspetjournals.org at ASPET Journals on April 17, 2024

DMD Fast Forward. Published on June 17, 2011 as DOI: 10.1124/dmd.111.038588
This article has not been copyedited and formatted. The final version may differ from this version.

Introduction

Chronic opioid treatment is associated with undesirable effects such as tolerance, addiction, respiratory depression, and constipation. These side effects of opioid treatment, especially respiratory depression, are more prevalent at the μ opioid receptor, although they are mediated by all three opioid receptors (μ, δ, and κ) (Le Merrer et al., 2009). Thus, a selective μ-opioid receptor antagonist may be useful for treatment of opioid overdose.

The μ opioid receptor (MOR) antagonists currently marketed for the treatment of excessive opiate-mediated side effects (especially respiratory depression) exhibit minimal selectivity for MOR over the κ and δ opioid receptors. In addition to their anti-analgesic effects, MOR antagonists can also improve drug dependence of other dependence-producing substances such as nicotine and alcohol (Bidlack and Mathews, 2009). Naltrexone is one of the early-discovered opioid antagonists that is devoid of agonist activity at the MOR. It has recently been demonstrated that two novel N-heterocyclic derivatives of naltrexone, NAP (17-cyclopropylmethyl-3,14β-dihydroxy-4,5α-epoxy-6β-[(4'-pyridyl)acetamido]morphinan) and NAQ (17-cyclopropylmethyl-3,14β-dihydroxy-4,5α-epoxy-6α-[(3'-isoquinolyl) acetamido]morphinan) (Figure 1), exhibited high selectivity for MOR relative to naltrexone. Both compounds also exhibited comparable antagonistic activity at the MOR and insignificant agonistic activity (Li et al., 2009). These results piqued interest in the potential clinical use of NAP and NAQ.

Downloaded from dmd.aspetjournals.org at ASPET Journals on April 17, 2024

DMD Fast Forward. Published on June 17, 2011 as DOI: 10.1124/dmd.111.038588
This article has not been copyedited and formatted. The final version may differ from this version.

Naltrexone and naloxone are currently used opioid antagonists bearing structural similarity to NAP/NAQ. In naloxone, the cyclopropyl group of naltrexone is substituted by an allyl group. Naltrexone is used orally as maintenance therapy for treating alcohol addiction and opioid addiction. In contrast to naltrexone, naloxone is primarily used as an emergency measure for parenterally treating opioid overdose. It is also used in combination with opioid agonists such as buprenorphine, oxycodone for treating opioid induced constipation. Both naltrexone and naloxone exhibit high first pass metabolism with bioavailability being ~5-40% and ~3% respectively (Fishman et al., 1973; Weinstein et al., 1973; Wall et al., 1981). The primary metabolite of naltrexone is 6β-naltrexol with minor metabolites being 2-hydroxy-3-O-methyl-6β-naltrexol, and 6β-naltrexone glucuronide (Wall et al., 1981). In both NAP and NAQ, the metabolically labile ketone group at position 6 of naltrexone has been substituted by an amide bond (Figure 1). As amides are hydrolytically and metabolically stable, the hypothesis is that NAP and NAQ will undergo less metabolism than naltrexone, at least at position 6. However, the prediction of metabolic stability is not necessarily straightforward, since both NAP and NAQ contain additional aromatic rings, which may make them more susceptible to aromatic hydroxylation.

The overall aim of this study was to obtain a preliminary assessment of the gastrointestinal absorption and hepatic metabolism of the two novel compounds, NAP and NAQ, with the ultimate goal of determining their potential as therapeutic agents. This is important since naltrexone exhibits high hepatic first-pass (oxidative and conjugative) metabolism resulting in low oral bioavailability and a short systemic half-life. A more selective MOR antagonist with

Downloaded from dmd.aspetjournals.org at ASPET Journals on April 17, 2024

DMD Fast Forward. Published on June 17, 2011 as DOI: 10.1124/dmd.111.038588
This article has not been copyedited and formatted. The final version may differ from this version.

higher oral bioavailability and a longer half-life would hold significant therapeutic advantages over currently available therapies such as naltrexone.

Downloaded from dmd.aspetjournals.org at ASPET Journals on April 17, 2024

DMD Fast Forward. Published on June 17, 2011 as DOI: 10.1124/dmd.111.038588
This article has not been copyedited and formatted. The final version may differ from this version.

Materials and Methods

Materials

NAP and NAQ were synthesized as previously described (Li et al., 2009). The Caco-2 cells were obtained from American Type Culture Collection (Manassas, VA). The MDCKII-MDR1 cell line was a generous donations from Dr. Piet Borst (Netherlands Cancer Institute, Amsterdam). Human liver microsomes (HLM; pooled from 200 patients, mixed gender) were obtained from Xenotech LLC (Lenexa, KS). Saccharo-1,4-lactone monohydrate was purchased from Calbiochem (San Diego, CA). GF120918 (elacridar) was purchased from Toronto Research Chemicals (Toronto, Canada). All other reagents and supplies were obtained commercially.

Cell culture and Bidirectional Transport

Caco-2 and MDCKII-MDR1 cells were cultured as previously described (Evers et al., 2000; Young et al., 2006). Cells were sub-cultured within 6-7 days for the Caco-2 cells, and 3-4 days for the MDCKII-MDR1 cells.

Caco-2 cells (passage numbers 39-45) and MDCKII-MDR1 cells (passage numbers 3-5) were used to study the directionality of NAP and NAQ transport. Cells were seeded onto 12-well transwell inserts (0.4 μM pore size) at a density of 80,000 cells/cm^2 for the Caco-2 cells and 50,000 cells/ cm^2 for the MDCKII-MDR1 cells, respectively. Bidirectional transport studies were conducted between days 20-25 for the Caco-2 cells and on day 6 for the MDCKII-MDR1 cells.

Transport studies were carried out in Hank's Balanced Salt Solution (HBSS) buffered with 10 mM HEPES (pH 7.4)Monolayers were incubated in transport buffer at 37ºC (50 r.p.m.) for 20 min (pre-equilibration period). The solutions were then aspirated off and the cells were treated

Downloaded from dmd.aspetjournals.org at ASPET Journals on April 17, 2024

DMD Fast Forward. Published on June 17, 2011 as DOI: 10.1124/dmd.111.038588
This article has not been copyedited and formatted. The final version may differ from this version.

with NAP/NAQ (10 µM) in the apical chamber for apical-to-basolateral studies, and in the basolateral chamber for basolateral-to-apical studies. All solutions were prepared in HBSS and the vehicle concentration was <0.5% v/v. Experiments where the effect of the P-gp inhibitor GF120918 (2 µM) were tested, were set up in the same way, except that the inhibitor was added to both chambers, during both pre-equilibration and experimental periods. Aliquots (200 µL) were removed from the receiver chambers at pre-determined time points (up to 2 hours), and replaced with an equal volume of transport buffer (37ºC). Acetonitrile (25 µL) was added to the withdrawn samples and centrifuged at 2500 x g for 10 min at 4ºC. A portion of the supernatant was used for analysis by HPLC-UV.

The integrity of the monolayer was assessed by determining the permeability of Lucifer Yellow (100 µM) for 30 minutes following transport of NAP/NAQ (Inokuchi et al., 2009). Results were used only from monolayers for which the apparent permeability coefficient of Lucifer Yellow was less than 1.0×10^{-6} cm/sec.

Following Lucifer Yellow transport, cells were lysed to determine intracellular concentrations of NAP/NAQ. Cells were washed once in transport medium, and ice-cold methanol (500 µL) was added to each transwell. Transwells were stored on ice for 15 min. Cells were scraped and sonicated for 10 min for further disruption. Following centrifugation at 2500 x g for 10 min, a portion of the supernatant was evaporated to dryness, reconstituted in 1:8 acetonitrile:transport buffer, and analyzed by HPLC-UV.

Metabolic stability of NAP and NAQ

Oxidation

Downloaded from dmd.aspetjournals.org at ASPET Journals on April 17, 2024

DMD Fast Forward. Published on June 17, 2011 as DOI: 10.1124/dmd.111.038588
This article has not been copyedited and formatted. The final version may differ from this version.

As metabolites of NAP/NAQ were unknown at this stage, disappearance of the substrates was monitored by HPLC-UV (232 nm). Reactions were initially optimized so that they were linear with respect to protein concentration and time. NAQ (0.5-80 µM) and NAP (0.5-30 µM) were added to 50 mM potassium phosphate buffer (pH 7.4) containing 3 mM $MgCl_2$, and the mixture was stored on ice. Reduced nicotinamide adenine dinucleotide phosphate (NADPH) generating system (5 mM glucose-6-phosphate, 1 mM nicotinamide adenine dinucleotide phosphate, and 1 U/mL glucose 6 phosphate dehydrogenase in 50 mM phosphate buffer, pH 7.4) was added to this mixture, and the components were warmed at 37ºC for 2 min. The reactions were initiated by adding human liver microsomes (HLM) to a final concentration of 0.5 mg/mL (total reaction volume 400 µL) for NAQ and 1 mg/mL for NAP (total reaction volume 250 µL). Reactions were carried out at 37ºC in a shaking water bath (90 r.p.m), with tubes open to the humidified atmosphere. Aliquots (50 µL) were withdrawn at predetermined time points (0, 15, 30, 45, 60, and 120 min for NAQ and 0, 15, 30, and 45 min for NAP) into an equal volume of ice-cold acetonitrile. The mixture was centrifuged at 2500 x g for 10 min at 4ºC. A portion of the supernatant was withdrawn and was evaporated to dryness under vacuum. The samples were reconstituted in 90:10 0.05% trifluoroacetic acid in water:acetonitrile. Phenacetin (80 µM) de-ethylation was utilized as a positive control for Phase 1 oxidative enzyme activity in the assays (0.5 mg/mL HLM). Control experiments contained DMSO in place of NAP/NAQ.

Glucuronidation

Since glucuronidation is known to be a major metabolic pathway for opioid compounds including naltrexone (Wall et al., 1981; Lotsch, 2005), we determined to study the extent to which NAP and NAQ may be glucuronidated. Glucuronidation of NAP and NAQ (0.5-100 µM

Downloaded from dmd.aspetjournals.org at ASPET Journals on April 17, 2024

DMD Fast Forward. Published on June 17, 2011 as DOI: 10.1124/dmd.111.038588
This article has not been copyedited and formatted. The final version may differ from this version.

and 1-100 µM respectively) were examined in human liver microsomes in the presence of uridine diphosphate-glucuronic acid (UDPGA, 3 mM), 0.5 mg/mL microsomal protein, alamethicin (50 µg/mL of microsomal protein), saccharolactone (6 mM), magnesium chloride (10 mM), Tris.HCl buffer, pH 7.4 (50 mM). Reactions were initiated by the addition of UDPGA, and were carried out at 37ºC in a shaking water bath (90 r.p.m). 17β-estradiol (50 µM) was used as the positive control for glucuronidation activity. The total reaction volume was 300 µL. Aliquots of 50 µL were withdrawn at 0, 0.5, 1, and 2 h into equal volumes of 6% trifluoroacetic acid. The tubes were centrifuged at 2,500 x g for 10 min at 4 ΄C. Aliquots of the supernatant were withdrawn and analyzed by HPLC-UV for NAP/NAQ, HPLC-UV for naltrexone and HPLC-fluorescence for estradiol, as outlined below. Control experiments contained DMSO in place of NAP/NAQ.

Identification of the oxidative metabolite of NAQ

The analytical method was successful in monitoring the time-dependent appearance of an oxidative metabolite of NAQ (M1). To identify this metabolite, several reaction mixtures were set up each containing NAQ at a final concentration of 1 µM (HLM at 0.5 mg/mL, total reaction volume 400 µL). Tubes were incubated under conditions that facilitated oxidative metabolism as outlined earlier, and prepared for HPLC-UV analysis, as outlined below. Fractions containing M1 were collected, evaporated to dryness, and reconstituted in 50:50 water containing 0.1% formic acid:ACN. NAQ (50 µg/mL) was prepared fresh in 50:50 water containing 0.1% formic acid:ACN.

Downloaded from dmd.aspetjournals.org at ASPET Journals on April 17, 2024

DMD Fast Forward. Published on June 17, 2011 as DOI: 10.1124/dmd.111.038588
This article has not been copyedited and formatted. The final version may differ from this version.

Standards and HPLC fractions were analyzed under the same conditions. They were directly infused onto a Micromass ZMD single quadrupole mass spectrometer, and analyzed by electrospray ionization (positive mode). Ionization conditions were as follows: capillary voltage (4.27 V), cone voltage (20 V), source block temperature (120 ºC), desolvation temperature (150 ºC). Signals were compared to analogous infusions with the same solvent system to determine unique ions associated with NAP, NAQ, and their metabolites.

HPLC analysis

Samples were maintained at 4ºC during analysis. The analytical column was a C18 column (Alltima HP C18, 4.6 mm x 100 mm, 3 µm (Alltech/Grace Davison, Deerfield, IL)). The mobile phase consisted of 0.05% trifluoroacetic acid in water (A) and acetonitrile (B), and was delivered at a flow rate of 1 mL/min.

For transport assay samples, the initial mobile phase composition was 90:10 A:B and was held at this composition for 1 min. The mobile phase composition was ramped to 50:50 over the next 6 min, changed to 90:10 A:B over the next minute, and held at 90:10 A:B for 3 min. NAP and NAQ were detected at 232 nm, while naltrexone was detected at 281 nm. Analytes were quantified from standard curves prepared in transport buffer:ACN (8:1). Calibration curves for NAP, NAQ, and naltrexone were all linear in the range 0.05-5 µM (R^2= 0.999). Samples from the oxidative metabolism studies of NAP and NAQ, were analyzed using the same method as above, except that the standards were prepared in 90:10 A:B.

Downloaded from dmd.aspetjournals.org at ASPET Journals on April 17, 2024

DMD Fast Forward. Published on June 17, 2011 as DOI: 10.1124/dmd.111.038588
This article has not been copyedited and formatted. The final version may differ from this version.

Analysis of samples from the glucuronidation studies of NAP, NAQ, naltrexone, and estradiol were performed as outlined below. The initial mobile phase composition was 99:1 A:B. It was held at this composition for 1 min, ramped to 91:9 and 45:55 over the next 2 and 6 mins. The composition was changed to 99:1 over 3 min, and allowed to equilibrate at 99:1 for another 3.5 min. Standards were prepared in deionized water. NAP, NAQ, and naltrexone were detected by UV at 232, 232, and 281 nm respectively, in accordance with their UV absorption peaks. Estradiol, estradiol 3-glucuronide, and estradiol 17-glucuronide were detected by fluorescence (275 nm/315 nm). Calibration curves for NAP, NAQ, naltrexone, and estradiol were linear in the range 0.5-100 µM (R^2= 0.999), 0.1-50 µM (R^2= 0.999), 5-5000 µM (R^2= 1.000), and 0.5-25 µM (R^2= 0.997).

Acetaminophen and phenacetin were detected at 240 nm. The analytical method for separating phenacetin and acetaminophen used the same mobile phase solvents as follows: 95:5 A:B for 1 min, ramped up to 70:30 over 4 min, ramped down to 95:5 over 4 min, and held at 95:5 for 3 min. Calibration curves for acetaminophen and phenacetin were linear in the range 0.05-5 µM (R^2= 0.999), and 0.25-25 µM (R^2= 0.999).

Human Plasma Protein Binding

Plasma samples from four healthy tobacco-free human subjects (3 male, 1 female) were obtained from BioChemed (Winchester, VA). Plasma samples were spiked with NAQ (10µM), NAP (10µM), ^{3}H-gentamicin (0.3µCi, as a low-binding control) or ^{3}H-2-methoxyestradiol (0.05µCi, as a high-binding control) and dialyzed against phosphate-buffered saline (pH 7.4) at 37°C using the Rapid Equilibrium Device (ThermoPierce) as previously described (Gulati et al., 2009) for

Downloaded from dmd.aspetjournals.org at ASPET Journals on April 17, 2024

DMD Fast Forward. Published on June 17, 2011 as DOI: 10.1124/dmd.111.038588
This article has not been copyedited and formatted. The final version may differ from this version.

20 hours to ensure equilibrium. Plasma and buffer samples (200µL) were mixed with 200µL buffer or plasma (respectively), and 600µL acetonitrile containing 0.01N HCl, vortexed, chilled, centrifuged, evaporated, reconstituted with 60µL mobile phase, and centrifuged again. Then 30µL of the supernatant were injected into the HPLC system described above but using an Agilent Microsorb-MV 3µ C18 100 x 4.6mm column. NAP was eluted at 40°C using 25% methanol 75% aqueous (20mM trifluoroacetic acid, 10mM triethylamine) with detection at 270nm. NAQ was eluted at 40°C using 55% methanol 75% aqueous with detection at 232nm. Standard curves were linear (r^2>0.99) between 0.08 to 20µM or 0.04 to 20µM for NAP and NAQ, respectively.

Data Analysis

Permeability calculations

The following equation was used to calculate apparent permeability in either the apical to basolateral direction ($P_{app, A-B}$) or basolateral to apical direction ($P_{app, B-A}$) :

$$P_{app} = dC/dt \times V_r/A \times C_d$$

Where dC/dt is the change in concentration in the receiver chamber with respect to time, V_r is the volume of the receiver chamber, A is the growth surface area, and C_d is the dosing concentration of the drug in the donor compartment.

Permeability directional ratio (PDR) was calculated as follows (Young et al., 2006):

$$PDR = P_{app, B-A}/ P_{app, A-B}$$

Metabolism calculations

Downloaded from dmd.aspetjournals.org at ASPET Journals on April 17, 2024

DMD Fast Forward. Published on June 17, 2011 as DOI: 10.1124/dmd.111.038588
This article has not been copyedited and formatted. The final version may differ from this version.

The oxidation and glucuronidation rates of NAP and NAQ were determined by the method of initial rates (Copeland, 2000). Plots of initial reaction rates (pmol/min/mg protein) vs. substrate concentration (μM) were fitted by the Michaelis-Menten (MM) equation (GraphPad Prism Software, version 5, La Jolla, CA), to estimate K_m and V_{max}, where, V_{max} is the maximal rate of oxidation/glucuronidation and is expressed in pmol/min/mg protein, and K_m is the substrate concentration at the half-maximal reaction rate. The MM parameter estimates were used to estimate the intrinsic clearance Cl_{int} (Cl_{int} = V_{max}/K_m). Cl_{int} was extrapolated using scaling methods to the *in vivo* clearance (CL_{int}^{total} (IVIVE)) expected in a healthy 75 kg individual, with the help of the following equation (i) (Naritomi et al., 2001):

$$CL_{\text{int}}(IVIVE) = \frac{V_{\max}}{K_m} \cdot \frac{52.5\, g\ microsomes}{g\ liver} \cdot \frac{20\, g\ \ liver}{kg\, body\, weight} \quad \text{.....(i)}$$

Units of CL_{int} (IVIVE) are in mL/min/kg. IVIVE represents *In Vitro In Vivo* Extrapolation.

With the values obtained from equation (i) the in vivo hepatic clearance (CL_{hep}) was estimated as follows (Naritomi et al., 2001):

$$CL_{\text{hep}} = \frac{fu * CL_{\text{int}}(IVIVE) * Q_{hep}}{fu * CL_{\text{int}}(IVIVE) + Q_{hep}} \quad \text{.....(ii)}$$

Where, f_u is unbound fraction of the compound in plasma (determined as above), and Q_{hep} is the hepatic blood flow rate (1500 mL/min).

Downloaded from dmd.aspetjournals.org at ASPET Journals on April 17, 2024

DMD Fast Forward. Published on June 17, 2011 as DOI: 10.1124/dmd.111.038588
This article has not been copyedited and formatted. The final version may differ from this version.

Results

Bidirectional transport of NAP and NAQ in Caco-2 cells

The apical-to-basolateral and basolateral-to-apical transport of NAP and NAQ were examined in Caco-2 cells to obtain an estimate of the human gastrointestinal absorption potential of these two compounds, and to assess whether or not they are subject to efflux transporters. Appearance of NAP, NAQ, and naltrexone in the receiver chamber as a function of time, was linear up to 2 h, the final time point of this study (supplemental Figure S1). The integrity of the Caco-2 monolayers was validated by estimating the apparent permeability coefficient (P_{app}) of Lucifer Yellow in the apical to basolateral, and basolateral to apical directions following transport of the compound of interest. Lucifer Yellow is a well-known endothelial cell permeability marker, but is also used as a paracellular permeability marker in epithelial cells (Young et al., 2006). The cutoff for an intact monolayer was set at an apparent permeability coefficient of (1×10^{-6} cm/sec) for Lucifer Yellow. Apparent permeability constants are reported in Table 1, including only data from monolayers judged to be intact from Lucifer Yellow permeability ($<1 \times 10^{-6}$ cm/sec). Permeability directional ratio (PDR) values $\geq$ 2.0 indicate net apical secretion ("efflux" transport) .

As shown in Table 1, the absorptive (A to B) permeability of NAQ was approximately 4-5 fold lower than that of caffeine, which is a highly permeable compound, and undergoes complete absorption in humans (Yazdanian et al., 1998). This is in contrast to NAP which exhibits an apparent absorptive permeability coefficient similar to that of mannitol, which is a marker of low permeability or paracellular permeability. The permeability of NAQ in the absorptive direction was approximately 4.5 fold greater than that of NAP, and was closer to that of naltrexone.

Downloaded from dmd.aspetjournals.org at ASPET Journals on April 17, 2024

DMD Fast Forward. Published on June 17, 2011 as DOI: 10.1124/dmd.111.038588
This article has not been copyedited and formatted. The final version may differ from this version.

NAQ also bears other similarities to naltrexone in that for both compounds the PDR was less than 2, suggesting that neither is an efflux transporter substrate (Giacomini et al., 2010). In contrast, NAP exhibited a PDR substantially greater than 2, indicating efflux transport. Efflux transporters expressed on the apical membrane of Caco-2 cells include P-glycoprotein (P-gp), breast cancer resistance protein (BCRP), and multidrug resistance-associated protein 2 (MRP2) (Englund et al., 2006; Seithel, 2006). GF120918 is a commonly utilized efflux transporter inhibitor that abrogates efflux mediated by P-gp as well as by BCRP (IC_{50} = 0.3 µM and 20 µM respectively) (Maliepaard et al., 2001; Matsson et al., 2009)). GF120918 reduced the PDR of digoxin, a well known P-gp substrate, from 5.1 to 1.2, confirming its inhibitory potential in our experimental setup (Table 1). Utilized at the same concentration (2 µM), GF120918 decreased the PDR of NAP to < 2, suggesting that the high PDR, and thus the efflux transport, of NAP is mainly due to P-gp, although contributions from other apical transporters such as BCRP (or a basolateral transporter) cannot yet be ruled out.

Bidirectional transport of NAP in MDCK-MDR1 cells

To confirm that NAP is a P-gp substrate, its bidirectional transport was estimated in MDCKII-MDR1 cells over-expressing human P-gp. In these cells, NAP exhibited a very high PDR, which was abolished in the presence of GF120918 (Table 2). This confirmed that NAP is a P-gp substrate. In contrast to the results from Caco-2 cells, the PDR reduction in the presence of GF120918 resulted from a much greater increase in P_{app} in the apical to basolateral direction compared to the decrease observed in the basolateral to apical direction.

Downloaded from dmd.aspetjournals.org at ASPET Journals on April 17, 2024

DMD Fast Forward. Published on June 17, 2011 as DOI: 10.1124/dmd.111.038588
This article has not been copyedited and formatted. The final version may differ from this version.

Plasma Protein Binding

Mass balance of both compounds between plasma and dialyzate was not significantly different from 100%, indicating good stability. Fraction unbound estimates for gentamicin and 2-methoxyestradiol, as low and high binding controls, were similar to previously reported values (Lakhani et al., 2006; Lexi-Comp, 2011). The unbound fraction in human plasma for NAP was 0.85 ±0.12, while that of NAQ was 0.026 ±0.012. Correspondingly, these data indicate that NAP is 15% bound, while NAQ is 97% bound.

Oxidative metabolism of NAQ and NAP

Phenacetin is a substrate of CYP1A2 and undergoes de-ethylation to form acetaminophen (Venkatakrishnan et al., 1998; Walsky, 2004). When HLM were incubated with phenacetin (80 µM), the analytical method was successfully able to monitor the appearance of acetaminophen (supplemental Figure S2), indicating that the experimental setup facilitated oxidative metabolism. The pooled human liver microsomes had already been certified by the vendor to be active for the major drug metabolizing enzymes (CYP1A2, CYP2C9, CYP2D6, CYP3A4). CYP1A2 was favored as an in-house positive control over the other enzymes due to the ease of availability of acetaminophen, the O-de-ethylation product of phenacetin. As the metabolites of NAP and NAQ were unknown at this stage, we monitored the disappearance of NAP or NAQ, rather than appearance of metabolites. Figures 2A and 2B show representative curves obtained at 0.5 µM and 80 µM NAQ, the lowest and highest concentrations of NAQ used. Regression analysis of the linear portion of the curves (120 min at 80 µM and 45 min at all other concentrations) returned the initial reaction velocities at each of these concentrations. Similarly, oxidation of NAP was examined in the concentration range 0.5-30 µM (Figures 3A and 3B) and

Downloaded from dmd.aspetjournals.org at ASPET Journals on April 17, 2024

DMD Fast Forward. Published on June 17, 2011 as DOI: 10.1124/dmd.111.038588
This article has not been copyedited and formatted. The final version may differ from this version.

regression analysis was performed on the linear portion of the curves (45 min) to estimate initial reaction velocities. The initial reaction velocities were plotted vs. initial substrate concentration to obtain the kinetic constants K_m and V_{max} for NAQ (15.8±5.5 μM and 192±24 pmol/min/mg protein, respectively; Figure 2C) and NAP (1.8±1.5 μM and 8.1±1.4 pmol/min/mg protein, respectively; Figure 3C). Higher concentrations of NAP were also tested for their susceptibility to oxidative metabolism, but presumably due to sensitivity issues, loss of NAP was not observed at these high concentrations. NAP has a higher apparent affinity (~10 fold lower K_m) for microsomal oxidative enzymes in comparison to NAQ, but the V_{max} of oxidation of NAQ is much higher than that of NAP. Using the methods described above, intrinsic hepatic clearances were predicted to be 13 and 5 ml/min/kg for NAQ and NAP, respectively, thus predicting that of NAQ to be 2.5-fold greater than that of NAP, mainly due to the greater V_{max} for NAQ. At all concentrations, the amount of substrate lost is more for NAQ than NAP (Supplemental Material, Table S1). Combining these estimates with the experimental values for fraction unbound in human plasma (as described above), we obtained estimates of hepatic clearance for NAQ of 0.33 mL/min/kg and for NAP of 3.5 ml/min/kg – suggesting low hepatic extraction for both compounds. By comparison, the systemic clearance of naltrexone (presumably mainly due to hepatic extraction) is approximately 17 ml/min/kg (McEnvoy, 1999).

For NAQ, we observed the appearance of a new peak concomitantly with the disappearance of NAQ. The peak area of this presumed metabolite of NAQ (M1) increased linearly with incubation time (data not shown). The apparent Michaelis-Menten constant (K_m), for the formation of M1, was 77.9 ± 10.3 μM. This is in the range of the K_m value obtained from the disappearance of NAQ (15.8 ± 5.5 μM), and consistent with M1 being the primary metabolite of

Downloaded from dmd.aspetjournals.org at ASPET Journals on April 17, 2024

DMD Fast Forward. Published on June 17, 2011 as DOI: 10.1124/dmd.111.038588
This article has not been copyedited and formatted. The final version may differ from this version.

NAQ. In contrast, while the analytical method was able to capture the loss of NAP, we were not able to monitor the appearance of any new metabolite peak by UV absorbance at either 232 nm or 270 nm.

Glucuronidation of NAP and NAQ

One of the major known circulating metabolites of naltrexone is its phenolic glucuronide conjugate (glucuronidated at position 3; see Figure 1) (Ventura, 1988). Based on their structural similarity to naltrexone, it was hypothesized that NAP and NAQ may undergo glucuronidation at the aromatic hydroxyl group. Therefore, we exposed NAP and NAQ to glucuronidation reactions, as described above. Due to the unavailability of metabolite standards, we monitored the loss in peak areas of NAP and NAQ. Contrary to the hypothesis, neither NAP (1-100 µM) nor NAQ (0.5- 100 µM) underwent any detectable glucuronidation. Glucuronidation of naltrexone was evaluated over a wider concentration range (1-2500 µM). Naltrexone glucuronidation was observed in the concentration range 50-200 µM, ranging from 0.1-5.8 pmol/min/mg protein. Under the same conditions, the analytical method was successfully able to monitor loss of estradiol (10 µM) (supplemental Figure S3), and the appearance of the 3- and 17-glucuronic acid conjugates of estradiol (data not shown).

Identification of the oxidative metabolite of NAQ

For NAQ standard, the peak of highest intensity was observed at m/z of 498.73, which corresponds to the $[M+H]^+$ peak of NAQ. In the HPLC eluent fractions containing pure NAQ, highest peak intensities were observed at m/z 249.74 and 498.86. These correspond respectively to the double and single positively charged peaks of NAQ. For the metabolite fraction, the peak

Downloaded from dmd.aspetjournals.org at ASPET Journals on April 17, 2024

DMD Fast Forward. Published on June 17, 2011 as DOI: 10.1124/dmd.111.038588
This article has not been copyedited and formatted. The final version may differ from this version.

of highest m/z was 444.66, and corresponds to the single positively charged N-dealkylation product of NAQ. To facilitate fragmentation, the cone voltage was increased to 106 V. Fragmentation patterns of the peaks obtained at 498.86 and 444.66 were similar: for both, peaks were observed that corresponded to loss of 18, 22, and 38 m/z units. This indicates that the 444.66 molecular ion retains the same molecular structure as NAQ (except for the N-dealkylation), suggesting that the primary metabolite of NAQ is the N-dealkylated product.

Discussion

The results suggest that between NAP and NAQ, NAQ is expected to have superior absorption across the gastrointestinal epithelia and holds more promise as an oral drug candidate, assuming similar gastrointestinal solubility. If permeability were to be the rate-determining factor driving oral absorption, NAQ can be expected to have absorption similar to naltrexone. Permeability of NAP is not only lower than naltrexone, but is also similar to that of paracellular permeability markers. This could be a major obstacle for further development of NAP as a drug candidate intended for oral absorption. The comparatively lower permeability of NAP does not necessarily eliminate its promise as a therapeutic agent. Methylnaltrexone, a quaternary amine opioid antagonist, has poor permeation across the blood brain barrier. It is clinically used for reversing opioid-induced peripheral side effects without causing loss of analgesia, or without precipitation of withdrawal symptoms. NAP has the potential of having a similar clinical usage.

Interestingly, NAP was determined to be a P-gp substrate, while NAQ was not. In mice, NAP and NAQ were able to antagonize the effects of morphine, which is an agonist at MOR (Li et al., 2009). The dose at which NAP produced 50% of this effect was 10-fold higher than that of

Downloaded from dmd.aspetjournals.org at ASPET Journals on April 17, 2024

DMD Fast Forward. Published on June 17, 2011 as DOI: 10.1124/dmd.111.038588
This article has not been copyedited and formatted. The final version may differ from this version.

NAQ. Opioid receptors are prevalent in the brain (Le Merrer et al., 2009). It is likely that P-gp, which is expressed and is functional at the blood-brain barrier (Giacomini et al., 2010), limits distribution of NAP to the brain. In Caco-2 cells, naltrexone did not undergo efflux, as previously reported (Kanaan et al., 2009). Compared to naltrexone, NAP carries a substituted pyridinyl side chain at the 6-position through an amide linkage, replacing the ketone group on naltrexone. This may explain the difference in their efflux profiles, as structure-activity relationships of P-gp substrates indicate that increasing the number of hydrogen bond acceptors on a molecule increases its chances of being recognized as a substrate by P-gp (Hochman, 2006). More interesting are the different efflux patterns of NAP and NAQ: NAQ differs from NAP by the presence of an additional aromatic ring and by the placement of the aromatic nitrogen atom, as well as the stereochemistry of the side chain. While it is not possible to identify the exact reason of the difference in the efflux patterns of NAP and NAQ without molecular modeling experiments, possible reasons could be suboptimal distances between the hydrogen bond acceptors, and/or steric hindrance due to the additional aromatic ring (Hochman, 2006).

P-gp mediated efflux is expected to be an additional impediment to the development of NAP as a drug candidate. Inhibition experiments in Caco-2 cells suggest that the large PDR results from P-gp facilitating secretory transport rather than inhibiting absorptive transport; the inhibitor enhanced the absorptive transport only to a modest extent. Incidentally, this asymmetrical effect of P-gp has been observed previously with several other substrates (Troutman and Thakker, 2003). Thus, efflux by P-gp may not additionally hamper NAP's intestinal transport beyond its already low diffusional permeability. However, the intended pharmacological use of NAP and NAQ are as selective antagonists at the central μ opioid receptors, which necessitates their

Downloaded from dmd.aspetjournals.org at ASPET Journals on April 17, 2024

DMD Fast Forward. Published on June 17, 2011 as DOI: 10.1124/dmd.111.038588
This article has not been copyedited and formatted. The final version may differ from this version.

crossing the blood brain barrier, where P-gp is functional. It has been observed that for compounds which exhibit a high P-gp efflux ratio *in vitro*, brain penetration is a greater hurdle than intestinal permeation (Hochman, 2006). So while NAQ may easily cross the blood brain barrier (based upon its observed *in vitro* permeability), it may be a more daunting task for NAP. Furthermore, in MDCKII-MDR1 cells, NAP had a very high PDR, demonstrating its activity as a good P-gp substrate.

Naltrexone is extensively metabolized following oral administration with oral bioavailability being reported to be 5-40%. Major plasma metabolites of naltrexone in man following IV administration are 6β-naltrexol, and the conjugates of naltrexone and 6β-naltrexol (Wall et al., 1981), with highest systemic exposures after oral administration obtained for 6β-naltrexol and its conjugate. After oral administration the predominant plasma metabolite was the 6β-naltrexol conjugate (Wall et al., 1981). The conjugates of naltrexone and 6β-naltrexol are the glucuronic acid conjugates (Ventura et al., 1988) at position 3 (Figure 1). Reduction of naltrexone to 6β-naltrexol was observed only in cytosolic fractions, but not in microsomal fractions. Enzymes responsible for the metabolism of naltrexone to 6β-naltrexol are aldo-keto reductase (AKR) isoforms 1C4, 1C1, and 1C2 (Porter et al., 2000; Breyer-Pfaff and Nill, 2004; Tong et al., 2010). Both NAP and NAQ lack the ketone moiety at position 6 of the morphinan ring structure, and are hence not expected to be reduced to the corresponding alcohol. Instead both compounds have substituted amide bonds at that position. Amides are generally stable to hydrolysis. Based on this, we hypothesized that NAP-3-glucuronide and NAQ-3-glucuronide would be the primary metabolites of NAP and NAQ. Contrary to our expectations, NAP or NAQ were not detectably glucuronidated. We examined the glucuronidation of NAP and NAQ, at concentrations much

Downloaded from dmd.aspetjournals.org at ASPET Journals on April 17, 2024

DMD Fast Forward. Published on June 17, 2011 as DOI: 10.1124/dmd.111.038588
This article has not been copyedited and formatted. The final version may differ from this version.

lower than the K_m values reported for naltrexone; based on doses at which NAP/NAQ were administered to mice, their plasma concentration was estimated to be in the nM range (Li et al., 2009).

Both NAP and NAQ underwent modest loss of peak area under conditions that facilitated oxidative metabolism, with the percent of NAP metabolized being about half that of NAQ. This is in accordance with what has been reported before for other naltrexamine derivatives in human liver S9 fractions, which either did not undergo oxidative metabolism, or exhibited half lives of 100-300 min (Ghirmai et al., 2009). The primary oxidative metabolite of NAQ was the N-dealkylated product. Naltrexone itself is not known to undergo N-dealkylation *in vivo* but several other opioids such as buprenorphine, morphine, codeine, which bear structural similarity to naltrexone, do undergo N-dealkylation (Caraco et al., 1996; Kobayashi et al., 1998; Projean et al., 2003), although for most of them glucuronidation is the major route of metabolism. Even though the experimental conditions successfully monitored the loss of NAP, time-dependent appearance of any major metabolite was not observed. A more sensitive detection, such as a tandem MS system, could be employed to further identify the primary metabolites of NAP.

As mentioned previously, one of the primary circulating metabolites of naltrexone is 6β-naltrexol. The intrinsic clearance (V_{max}/K_m) for the formation of 6β-naltrexol from naltrexone in human liver cytosolic fractions has been reported to be 12.6 and 5-36.7 μL/min/mg protein (Porter et al., 2000; Tong et al., 2010). To obtain an estimate of the hepatic clearance (CL_{hep}), these values of intrinsic clearance were scaled up using the same method utilized for NAP and NAQ (Metabolism calculations in Data Analysis in Materials and Methods section). The

Downloaded from dmd.aspetjournals.org at ASPET Journals on April 17, 2024

DMD Fast Forward. Published on June 17, 2011 as DOI: 10.1124/dmd.111.038588
This article has not been copyedited and formatted. The final version may differ from this version.

unbound fraction of naltrexone in human plasma is 72-79% (McEnvoy, 1999). Therefore, the hepatic clearance (CL_{hep}) of naltrexone was estimated to be 3.2 -12.1 mL/min/kg. Using this extrapolative scaling approach, we speculate that the hepatic clearance for NAP (3.5 mL/min/kg) may be similar to naltrexone, while that of NAQ (0.33 mL/min/kg) is likely lower by an order of magnitude.

In conclusion, both NAP and NAQ have promise as new drug candidates. Selective μ-opioid receptor antagonists NAP and NAQ showed evidence of hepatic oxidative metabolism (NAQ>NAP) but no evidence of hepatic glucuronidation; NAP was found to be a P-gp substrate with low gastrointestinal permeability while NAQ showed better permeability and lacked activity as a P-gp substrate. Therefore, in contrast to NAP, NAQ would be suitable for oral absorption & penetration of the blood-brain barrier. Combining the improved MOR selectivity with its potential pharmacokinetic benefits, NAQ appears to be a good lead compound with advantages over naltrexone as a MOR antagonist.

Downloaded from dmd.aspetjournals.org at ASPET Journals on April 17, 2024

DMD Fast Forward. Published on June 17, 2011 as DOI: 10.1124/dmd.111.038588
This article has not been copyedited and formatted. The final version may differ from this version.

Acknowledgements

We acknowledge the following individuals: Joseph K. Ritter, Ph.D., Associate Professor, Department of Pharmacology and Toxicology, VCU, for assistance with Caco2 cell cultures and drug metabolism experiments; Michael Hindle, Ph.D., Research Associate Professor, Department of Pharmaceutics for providing access to his mass spectrometer and assistance in the interpretation of the results; Prajakta Badri, Ph.D., for extrapolating PK parameters of NAP and NAQ from in silico models; Fay K. Kessler, Research Assistant, Department of Pharmacology and Toxicology, VCU, for helping with technical issues with Caco-2 cell cultures.

Authorship Contributions

Participated in research design: Mitra, Venitz, Zhang, Gerk.

Conducted experiments: Mitra, Yuan, Gerk.

Contributed new reagents or analytic tools: Mitra, Yuan, Gerk.

Performed data analysis: Mitra, Venitz, Gerk.

Wrote or contributed to the writing of the manuscript: Mitra, Venitz, Zhang, Gerk.

Downloaded from dmd.aspetjournals.org at ASPET Journals on April 17, 2024

DMD Fast Forward. Published on June 17, 2011 as DOI: 10.1124/dmd.111.038588
This article has not been copyedited and formatted. The final version may differ from this version.

References

Bidlack JM and Mathews JL (2009) The chemistry and pharmacology of μ opioid receptors, in: *Opiate Receptors and Antagonists - From bench to the clinic* (Dean R, Bilsky EJ and Negus SS eds), pp 83, Humana Press.

Breyer-Pfaff U and Nill K (2004) Carbonyl reduction of naltrexone and dolasetron by oxidoreductases isolated from human liver cytosol. *J Pharm Pharmacol* **56:**1601-1606.

Caraco Y, Tateishi T, Guengerich FP and Wood AJ (1996) Microsomal codeine N-demethylation: cosegregation with cytochrome P4503A4 activity. *Drug Metab Dispos* **24:**761-764.

Copeland RA (2000) *Enzymes: a practical introduction to structure, mechanism, and data analysis*. New York: J. Wiley.

Englund G, Rorsman F, Roennblom A, Karlbom U, Lazorova L, Grasjoe J, Kindmark A and Artursson P (2006) Regional levels of drug transporters along the human intestinal tract: co-expression of ABC and SLC transporters and comparison with Caco-2 cells. *European Journal of Pharmaceutical Sciences* **29:**269-277.

Evers R, Kool M, Smith AJ, van Deemter L, de Haas M and Borst P (2000) Inhibitory effect of the reversal agents V-104, GF120918 and Pluronic L61 on MDR1 Pgp-, MRP1- and MRP2-mediated transport. *Br J Cancer* **83:**366-374.

Fishman J, Roffwarg H and Hellman L (1973) Disposition of naloxone-7,8,3H in normal and narcotic-dependent men. *J Pharmacol Exp Ther* **187:**575-580.

Ghirmai S, Azar MR and Cashman JR (2009) Synthesis and pharmacological evaluation of 6-naltrexamine analogs for alcohol cessation. *Bioorg Med Chem* **17:**6671-6681.

Downloaded from dmd.aspetjournals.org at ASPET Journals on April 17, 2024

DMD Fast Forward. Published on June 17, 2011 as DOI: 10.1124/dmd.111.038588
This article has not been copyedited and formatted. The final version may differ from this version.

Giacomini KM, Huang SM, Tweedie DJ, Benet LZ, Brouwer KL, Chu X, Dahlin A, Evers R, Fischer V, Hillgren KM, Hoffmaster KA, Ishikawa T, Keppler D, Kim RB, Lee CA, Niemi M, Polli JW, Sugiyama Y, Swaan PW, Ware JA, Wright SH, Wah Yee S, Zamek-Gliszczynski MJ and Zhang L (2010) Membrane transporters in drug development. *Nat Rev Drug Discov* **9:**215-236.

Gulati A, Boudinot FD and Gerk PM (2009) Binding of lopinavir to human alpha1-acid glycoprotein and serum albumin. *Drug Metab Dispos* **37:**1572-1575.

Hochman J (2006) Role of mechanistic transport studies in lead optimization, in: *Optimizing the drug-like properties of leads in drug discovery* (Ronald T. Borchardt EHK, Michael J. Hageman, Dhiren R. Thakker, James L. Stevens ed), pp 26-48, Springer.

Inokuchi H, Takei T, Aikawa K and Shimizu M (2009) The effect of hyperosmosis on paracellular permeability in Caco-2 cell monolayers. *Biosci Biotechnol Biochem* **73:**328-334.

Kanaan M, Daali Y, Dayer P and Desmeules J (2009) P-glycoprotein is not involved in the differential oral potency of naloxone and naltrexone. *Fundam Clin Pharmacol* **23:**543-548.

Kobayashi K, Yamamoto T, Chiba K, Tani M, Shimada N, Ishizaki T and Kuroiwa Y (1998) Human buprenorphine N-dealkylation is catalyzed by cytochrome P450 3A4. *Drug Metab Dispos* **26:**818-821.

Lakhani N, Sparreboom A, Venitz J, Dahut WL and Figg WD (2006) Plasma protein binding of the investigational anticancer agent 2-methoxyestradiol. *Anticancer Drugs* **17:**977-983.

Le Merrer J, Becker JA, Befort K and Kieffer BL (2009) Reward processing by the opioid system in the brain. *Physiol Rev* **89:**1379-1412.

Downloaded from dmd.aspetjournals.org at ASPET Journals on April 17, 2024

DMD Fast Forward. Published on June 17, 2011 as DOI: 10.1124/dmd.111.038588
This article has not been copyedited and formatted. The final version may differ from this version.

Lexi-Comp (2011) Gentamicin, Lexi-Comp Online.

Li G, Aschenbach LC, Chen J, Cassidy MP, Stevens DL, Gabra BH, Selley DE, Dewey WL, Westkaemper RB and Zhang Y (2009) Design, synthesis, and biological evaluation of 6alpha- and 6beta-N-heterocyclic substituted naltrexamine derivatives as mu opioid receptor selective antagonists. *J Med Chem* **52:**1416-1427.

Lotsch J (2005) Opioid metabolites. *J Pain Symptom Manage* **29:**S10-24.

Maliepaard M, Scheffer GL, Faneyte IF, van Gastelen MA, Pijnenborg AC, Schinkel AH, van De Vijver MJ, Scheper RJ and Schellens JH (2001) Subcellular localization and distribution of the breast cancer resistance protein transporter in normal human tissues. *Cancer Res* **61:**3458-3464.

Matsson P, Pedersen JM, Norinder U, Bergstrom CA and Artursson P (2009) Identification of novel specific and general inhibitors of the three major human ATP-binding cassette transporters P-gp, BCRP and MRP2 among registered drugs. *Pharm Res* **26:**1816-1831.

McEnvoy GK (1999) *AHFS Drug Information*. American Society of Health-System Pharmacists, Inc., Bethesda.

Naritomi Y, Terashita S, Kimura S, Suzuki A, Kagayama A and Sugiyama Y (2001) Prediction of human hepatic clearance from in vivo animal experiments and in vitro metabolic studies with liver microsomes from animals and humans. *Drug Metab Dispos* **29:**1316-1324.

Porter SJ, Somogyi AA and White JM (2000) Kinetics and inhibition of the formation of 6beta-naltrexol from naltrexone in human liver cytosol. *Br J Clin Pharmacol* **50:**465-471.

Downloaded from dmd.aspetjournals.org at ASPET Journals on April 17, 2024

DMD Fast Forward. Published on June 17, 2011 as DOI: 10.1124/dmd.111.038588
This article has not been copyedited and formatted. The final version may differ from this version.

Projean D, Morin PE, Tu TM and Ducharme J (2003) Identification of CYP3A4 and CYP2C8 as the major cytochrome P450 s responsible for morphine N-demethylation in human liver microsomes. *Xenobiotica* **33:**841-854.

Seithel A, Karlsson, J., Hilgendorf, C., Bjoerquist, A., Ungell, A. (2006) Variability in mRNA expression of ABC- and SLC-transporters in human intestinal cells: comparison between human segments and Caco-2 cells. *European Journal of Pharmaceutical Sciences* **28:**291-299.

Tong Z, Chandrasekaran A, Li H, Rotshteyn Y, Erve JC, Demaio W, Talaat R, Hultin T and Scatina J (2010) In vitro metabolism and identification of human enzymes involved in the metabolism of methylnaltrexone. *Drug Metab Dispos* **38:**801-807.

Troutman MD and Thakker DR (2003) Efflux ratio cannot assess P-glycoprotein-mediated attenuation of absorptive transport: asymmetric effect of P-glycoprotein on absorptive and secretory transport across Caco-2 cell monolayers. *Pharm Res* **20:**1200-1209.

Venkatakrishnan K, von Moltke LL and Greenblatt DJ (1998) Human Cytochromes P450 Mediating Phenacetin O-Deethylation in Vitro: Validation of the High Affinity Component as an Index of CYP1A2 Activity. *Journal of Pharmaceutical Sciences* **87:**1502-1507.

Ventura R, de la Torre R and Segura J (1988) Analysis of naltrexone urinary metabolites. *J Pharm Biomed Anal* **6:**887-893.

Wall ME, Brine DR and Perez-Reyes M (1981) Metabolism and disposition of naltrexone in man after oral and intravenous administration. *Drug Metab Dispos* **9:**369-375.

Walsky R, Obach, RS (2004) Validated assays for human cytochrome P450 activities. *Drug Metabolism and Disposition* **32:**647-660.

Downloaded from dmd.aspetjournals.org at ASPET Journals on April 17, 2024

DMD Fast Forward. Published on June 17, 2011 as DOI: 10.1124/dmd.111.038588
This article has not been copyedited and formatted. The final version may differ from this version.

Weinstein SH, Pfeffer M and Schor JM (1973) Metabolism and pharmacokinetics of naloxone. *Adv Biochem Psychopharmacol* **8:**525-535.

Yazdanian M, Glynn SL, Wright JL and Hawi A (1998) Correlating partitioning and caco-2 cell permeability of structurally diverse small molecular weight compounds. *Pharm Res* **15:**1490-1494.

Young AM, Audus KL, Proudfoot J and Yazdanian M (2006) Tetrazole compounds: the effect of structure and pH on Caco-2 cell permeability. *J Pharm Sci* **95:**717-725.

Downloaded from dmd.aspetjournals.org at ASPET Journals on April 17, 2024

DMD Fast Forward. Published on June 17, 2011 as DOI: 10.1124/dmd.111.038588
This article has not been copyedited and formatted. The final version may differ from this version.

Footnotes

This work was supported by the National Institutes of Health [grants DA024022 and MD002256], the Thomas F. and Kate Miller Jeffress Trust, and the VCU School of Pharmacy.

This work was presented in part at the 2010 Annual Meeting of the American Association of Pharmaceutical Scientists.

Reprint Requests:

Phillip M. Gerk, Pharm.D., Ph.D.

Dept. of Pharmaceutics, School of Pharmacy, Virginia Commonwealth University

410 N. 12th Street, PO Box 980533

Richmond, VA 23298-0533

phone: (804) 828-6321

fax: (804) 828-8359

email: pmgerk@vcu.edu

Downloaded from dmd.aspetjournals.org at ASPET Journals on April 17, 2024

DMD Fast Forward. Published on June 17, 2011 as DOI: 10.1124/dmd.111.038588
This article has not been copyedited and formatted. The final version may differ from this version.

Figure legends

Figure 1. Chemical structures of naltrexone, NAP, and NAQ.

Figure 2: Metabolism of NAQ in Human Liver Microsomes. In order to estimate the initial reaction velocities, HLM (0.5 mg/mL, total reaction volume of 400 µL) were incubated with NAQ (0.5-80 µM), and loss of NAQ was monitored as a function of time. Parts (**A**) and (**B**) represent the reaction profiles observed at 0.5 µM and 80 µM respectively. Panel **C**: Concentration-dependent oxidative metabolism of NAQ in HLM. HLM (0.5 mg/mL) were incubated with NAQ under conditions that facilitated oxidative metabolism. The initial reaction velocities at each concentration were plotted vs. the concentration. The curve was fitted by the Michaelis-Menten equation to estimate the kinetic constants K_m and V_{max} (see text). Data are plotted as mean ± S.D. (n=3).

Figure 3: Determination of initial reaction velocities from oxidative metabolism studies of NAP in HLM. In order to estimate the initial reaction velocities, HLM (1 mg/mL, total reaction volume 250 µL) were incubated with NAP (0.5-30 µM), and loss of NAP was monitored as a function of time. Parts (**A**) and (**B**) represent the reaction profiles observed at 0.5 µM and 30 µM respectively. Panel **C**: Concentration-dependent oxidative metabolism of NAP in HLM. HLM (0.5 mg/mL) were incubated with NAP under conditions that facilitated oxidative metabolism. The initial reaction velocities at each concentration were plotted vs. the concentration. The curve was fitted by the Michaelis-Menten equation to estimate the kinetic constants K_m and V_{max} (see text). Data are plotted as mean ± S.D. (n=3).

Downloaded from dmd.aspetjournals.org at ASPET Journals on April 17, 2024

DMD Fast Forward. Published on June 17, 2011 as DOI: 10.1124/dmd.111.038588
This article has not been copyedited and formatted. The final version may differ from this version.

Table 1: Bidirectional transport in Caco-2 cells

	P_{app} (x 10^6, cm/sec)		
	A to B	**B to A**	**PDR**
NAQ (10 µM)	2.85±0.66	4.24±1.04	1.5
NAP (10 µM)	0.6±0.17	7.8±1.0	13.1
NAP (10 µM) + GF120918 (2 µM)	0.8±0.2	1.32±0.13	1.6
Naltrexone (10 µM)	4.39±1.22	3.7±0.96	0.8
Caffeine (100 µM)	10.2±3.2	11.4±2.6	1.1
Mannitol (3 µM)	0.51±0.05	0.67±0.05	1.3
Digoxin (0.10 µM)	1.05±0.17	5.3±0.38	5.1
Digoxin + GF120918 (2 µM)	1.62±0.29	1.89±0.09	1.2

Apparent permeability coefficients (P_{app}) of substrates were determined by incubating Caco-2 monolayers with substrate at 37ºC for 2 hours. P_{app} was determined in the apical to basolateral (A to B), as well as, basolateral to apical (B to A) directions. PDR = Permeability directional ratio = $P_{app, B\ to\ A}/P_{app, A\ to\ B.}$ Data represent mean ± S.D.

Downloaded from dmd.aspetjournals.org at ASPET Journals on April 17, 2024

DMD Fast Forward. Published on June 17, 2011 as DOI: 10.1124/dmd.111.038588
This article has not been copyedited and formatted. The final version may differ from this version.

Table 2: Bidirectional transport of NAP in MDCK-MDR1 cells

	P_{app} (x 10^6, cm/sec)		PDR
	A to B	**B to A**	
NAP (10 μM)	0.037±0.024	12.5±1.9	341
NAP (10 μM) + GF120918 (2 μM)	1.5±0.5	3.3±0.12	2.1

The apparent permeability coefficients (P_{app}) of NAP were determined by incubating MDCK-MDR1 monolayers with NAP (10 μM) at 37ºC for 2 hours. P_{app} was determined in the apical to basolateral (A to B), as well as, basolateral to apical (B to A) directions. PDR = Permeability directional ratio = $P_{app, B\ to\ A}/P_{app, A\ to\ B.}$ Data represent mean ± S.D.

Downloaded from dmd.aspetjournals.org at ASPET Journals on April 17, 2024

DMD Fast Forward. Published on June 17, 2011 as DOI: 10.1124/dmd.111.038588
This article has not been copyedited and formatted. The final version may differ from this version.

Figure 1.

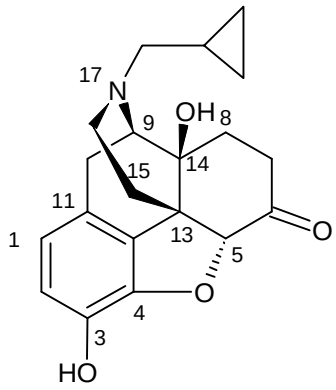

Naltrexone

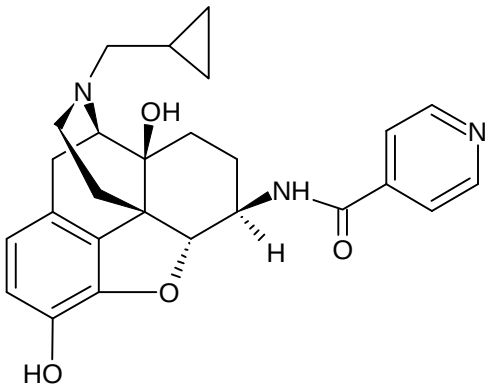

NAP

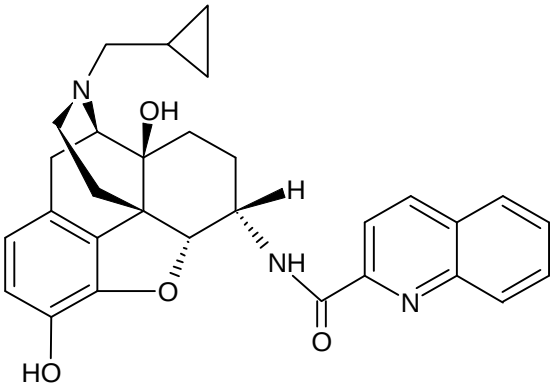

NAQ

Downloaded from dmd.aspetjournals.org at ASPET Journals on April 17, 2024

igure 2.

DMD Fast Forward. Published on June 17, 2011 as DOI: 10.1124/dmd.111.038588
This article has not been copyedited and formatted. The final version may differ from this version.

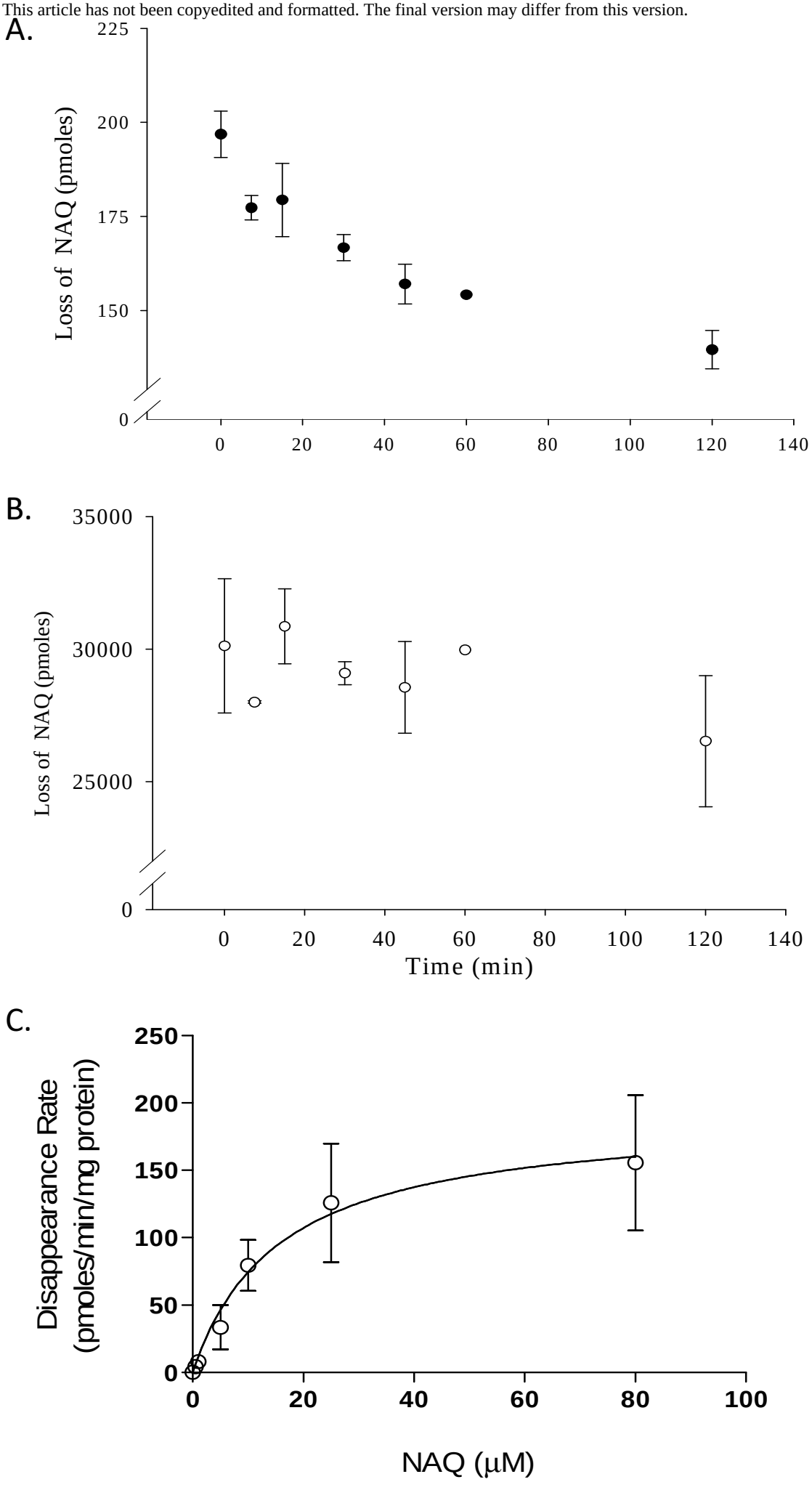

Downloaded from dmd.aspetjournals.org at ASPET Journals on April 17, 2024

igure 3.

DMD Fast Forward. Published on June 17, 2011 as DOI: 10.1124/dmd.111.038588
This article has not been copyedited and formatted. The final version may differ from this version.

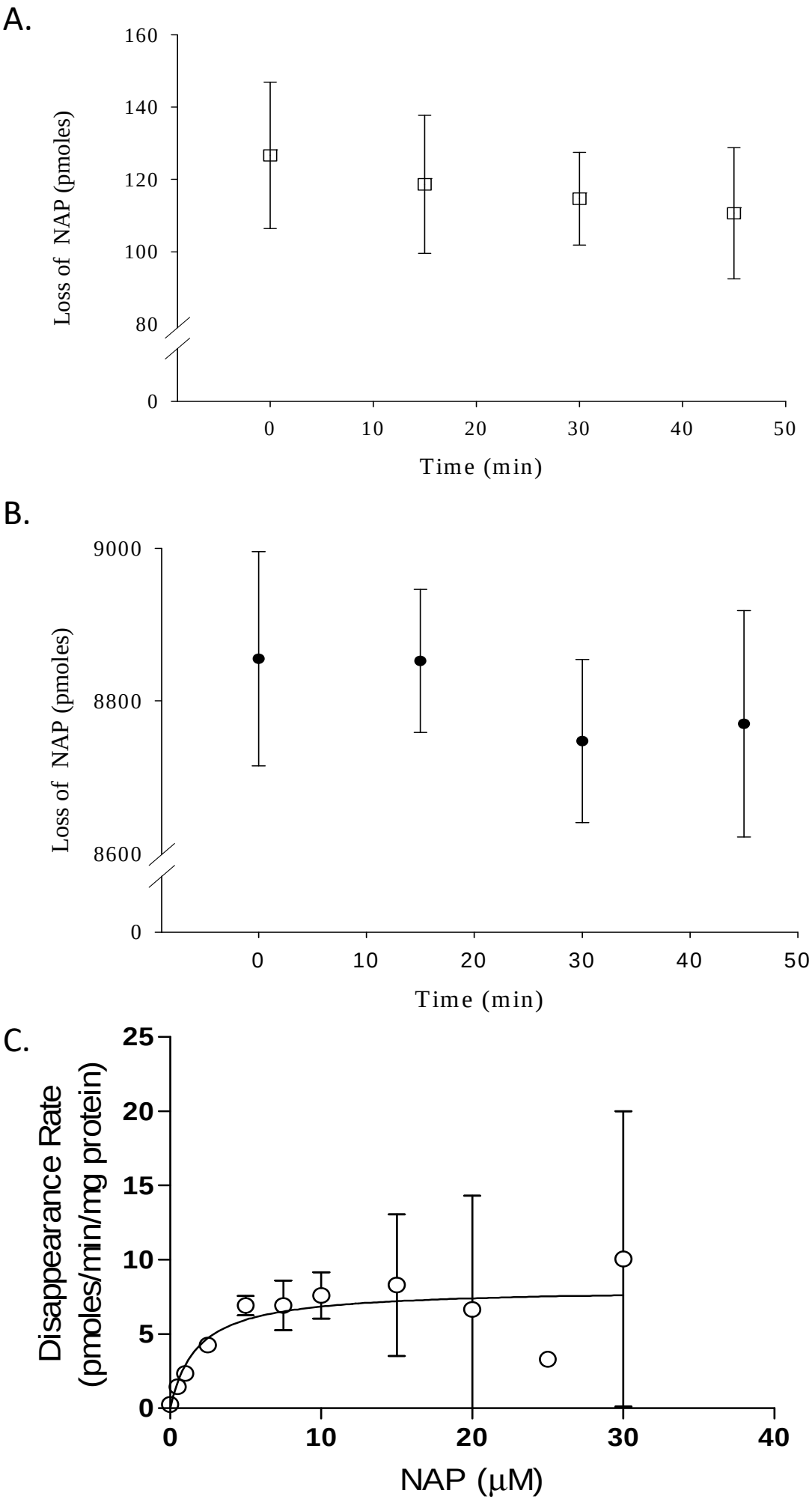

Downloaded from dmd.aspetjournals.org at ASPET Journals on April 17, 2024